

## INTEGRATED NEURAL FLIGHT AND PROPULSION CONTROL SYSTEM

John Kaneshige\* and Karen Gundy-Burlet†

Abstract

This paper describes an integrated neural flight and propulsion control system, which uses a neural network based approach for applying alternate sources of control power in the presence of damage or failures. Under normal operating conditions, the system utilizes conventional flight control surfaces. Neural networks are used to provide consistent handling qualities across flight conditions and for different aircraft configurations. Under damage or failure conditions, the system may utilize unconventional flight control surface allocations, along with integrated propulsion control, when additional control power is necessary for achieving desired flight control performance. In this case, neural networks are used to adapt to changes in aircraft dynamics and control allocation schemes. Of significant importance here is the fact that this system can operate without emergency or backup flight control mode operations. An additional advantage is that this system can utilize, but does not require, fault detection and isolation information or explicit parameter identification. Piloted simulation studies were performed on a commercial transport aircraft simulator. Subjects included both NASA test pilots and commercial airline crews. Results demonstrate the potential for improving handling qualities and significantly increasing survivability rates under various simulated failure conditions.

Introduction

In the last 30 years, at least 10 aircraft have experienced major flight control system failures claiming more than 1100 lives.<sup>1</sup> Following the DC-10 accident at Sioux City, Iowa in 1989, the National Transportation Safety Board recommended "research and development of backup flight control systems for newly certified wide-body airplanes that utilize an

alternate source of motive power separate from that source used for the conventional control system".<sup>2</sup> To investigate the possibility of using engine thrust for emergency flight control, NASA developed a Propulsion Controlled Aircraft (PCA) system that uses only augmented engine thrust for flight control. The concept was successfully flight tested on the F-15 airplane<sup>1</sup>, and MD-11 transport<sup>3</sup>, which included actual landings using PCA control.

In order to provide a full-time system capable of compensating for a broader spectrum of failures, NASA researchers began investigating techniques for integrating both flight and propulsion control. The concept was to develop a system capable of utilizing all remaining sources of control power after damage or failures. In order to adapt to varying levels of performance under different control allocation schemes, PCA technologies<sup>4</sup> were incorporated into a neural flight control architecture<sup>5</sup> developed as part of NASA's Intelligent Flight Control (IFC) program. The resulting Integrated Neural Flight and Propulsion Control System (INFPCS) uses a daisy-chain control allocation technique to ensure that conventional flight control surfaces will be utilized under normal operating conditions. Under damage or failure conditions, the system may allocate flight control surfaces, and incorporate propulsion control, when additional control power is necessary for achieving desired flight control performance.

The neural network based approach incorporates direct adaptive control with dynamic inversion to provide consistent handling qualities without requiring extensive gain-scheduling or explicit system identification. This particular architecture uses both pre-trained and on-line learning neural networks, and reference models to specify desired handling qualities. Pre-trained neural networks are used to provide estimates of aerodynamic stability and control characteristics required for model inversion. On-line learning neural networks are used to compensate for errors and adapt to changes in aircraft dynamics and control allocation schemes.

Piloted simulation studies were performed at NASA Ames Research Center on a commercial transport aircraft simulator. Subjects included both NASA test pilots and commercial airline crews. This paper contains a brief overview of the system architecture, and presents simulation results comparing the performance to conventional systems under nominal and simulated failure conditions.

\* Computer Engineer, Member AIAA, NASA Ames Research Center, Moffett Field, CA

† Research Scientist, NASA Ames Research Center, Moffett Field, CA

Copyright © 2001 by the American Institute of Aeronautics and Astronautics, Inc. No copyright is asserted in the United States under Title 17, U.S. Code. The U.S. Government has a royalty-free license to exercise all rights under the copyright claimed herein for Governmental purposes. All other rights are reserved by the copyright owner.

## Nomenclature

$h$	=	altitude, ft
$K_i$	=	error controller integral gain
$K_p$	=	error controller proportional gain
$p$	=	roll rate, rad/sec
$p_c$	=	roll rate command, rad/sec
$\dot{p}_c$	=	roll acceleration command, rad/sec <sup>2</sup>
$q$	=	pitch rate, rad/sec
$q_c$	=	pitch rate command, rad/sec
$\dot{q}_c$	=	pitch acceleration command, rad/sec <sup>2</sup>
$r$	=	yaw rate, rad/sec
$r_c$	=	yaw rate command, rad/sec
$\dot{r}_c$	=	yaw acceleration command, rad/sec <sup>2</sup>
$v_t$	=	true airspeed, ft/sec
$\alpha$	=	angle of attack, deg
$\beta$	=	sideslip, deg
$\delta_{ail}$	=	symmetric aileron command, deg
$\delta_{dail}$	=	differential aileron command, deg
$\delta_{rud}$	=	rudder command, deg
$\delta_{elev}$	=	symmetric elevator command, deg
$\delta_{thr}$	=	symmetric thrust command, deg
$\delta_{dthr}$	=	differential thrust command, deg
$\omega_e$	=	error controller frequency, rad/sec
$\omega_p$	=	roll rate reference model frequency, rad/sec
$\omega_q$	=	pitch rate reference model frequency, rad/sec
$\omega_r$	=	yaw rate reference model frequency, rad/sec
$\zeta_e$	=	error controller damping ratio

## System Architecture

The neural flight control architecture is based upon the augmented model inversion controller, developed by Rysdyk and Calise.<sup>6</sup> This direct adaptive tracking dynamic inverse controller, figure 1, integrates feedback linearization theory with both pre-trained and on-line learning neural networks. Pre-trained neural networks are used to provide estimates of aerodynamic stability and control characteristics required for model inversion. On-line learning neural networks are used to generate command augmentation signals to compensate for errors in the estimates and from the model inversion. The on-line learning neural networks also provide additional potential for adapting to changes in aircraft dynamics due to damage or failure. Reference models are used to filter command inputs in order to specify desired handling qualities. A Lyapunov stability proof guarantees boundedness of the tracking error and network weights.<sup>6</sup>

A daisy-chain control allocation technique is used to ensure that conventional flight control surfaces will be utilized under normal operating conditions. Under damage or failure conditions, the system may utilize unconventional flight control surface allocations, along with integrated propulsion control, when additional control power is necessary for achieving desired flight control performance. Of significant importance here is the fact that this system can operate without emergency or backup flight control mode operations. An additional advantage is that this system can utilize, but does not require, fault detection and isolation information or explicit parameter identification.

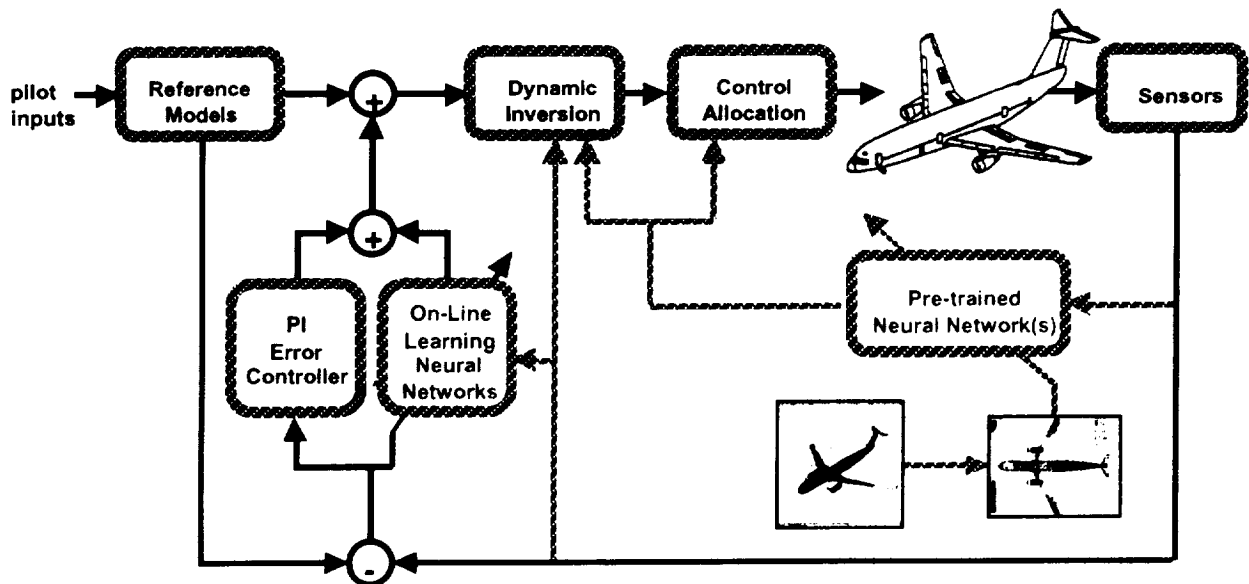


Figure 1. Neural Flight Control System

## Reference Models

The pilot commands roll rate and aerodynamic normal and lateral accelerations through stick and rudder pedal inputs. These commands are then transformed into body-axis rate commands, which also include turn coordination, level turn compensation, and yaw-dampening terms. First-order reference models are used to filter these commands in order to shape desired handling qualities. The roll rate, pitch rate, and yaw rate reference model frequencies ( $\omega_p$ ,  $\omega_q$ ,  $\omega_r$ ) used for this evaluation were 3.5, 2.5, and 2.0 rad/sec respectively. The filtered acceleration commands ( $\dot{p}_c$ ,  $\dot{q}_c$ ,  $\dot{r}_c$ ) are used for dynamic inversion. The filtered rates commands ( $p_c$ ,  $q_c$ ,  $r_c$ ) are used to compute tracking errors.

Alternate reference models can be applied to specify different handling qualities under damage or failure conditions. However static reference models were utilized in order to evaluate performance without reliance on degraded mode operations.

## Dynamic Inversion

Dynamic inversion is based upon feedback linearization theory. No gain-scheduling is required since gains are functions of aerodynamic stability and control derivative estimates and sensor feedback. To perform the model inversion, acceleration commands are used to replace the actual accelerations in the quasi-linear model

$$\begin{bmatrix} \dot{p} \\ \dot{q} \\ \dot{r} \end{bmatrix} = \hat{A}(x) \begin{bmatrix} p \\ q \\ r \end{bmatrix} + \hat{B}(x) \begin{bmatrix} \delta_{dail} \\ \delta_{elev} \\ \delta_{drud} \end{bmatrix} \quad (1)$$

The model is then inverted in order to solve for the necessary control surface commands

$$\begin{bmatrix} \delta_{dail} \\ \delta_{elev} \\ \delta_{drud} \end{bmatrix} = \hat{B}^{-1}(x) \left\{ \begin{bmatrix} \dot{p}_c \\ \dot{q}_c \\ \dot{r}_c \end{bmatrix} - \hat{A}(x) \begin{bmatrix} p \\ q \\ r \end{bmatrix} \right\} \quad (2)$$

## Pre-Trained Neural Network

A Levenberg-Marquardt (LM) multi-layer perceptron<sup>7</sup> is used to provide dynamic estimates for model inversion. The LM network is pre-trained with stability and control derivative data generated by a Rapid Aircraft Modeler (RAM), figure 2, and vortex-lattice code (VORVIEW), figure 3. In general, stability and control derivative estimates were achieved to within 10% of their actual values.<sup>8</sup>

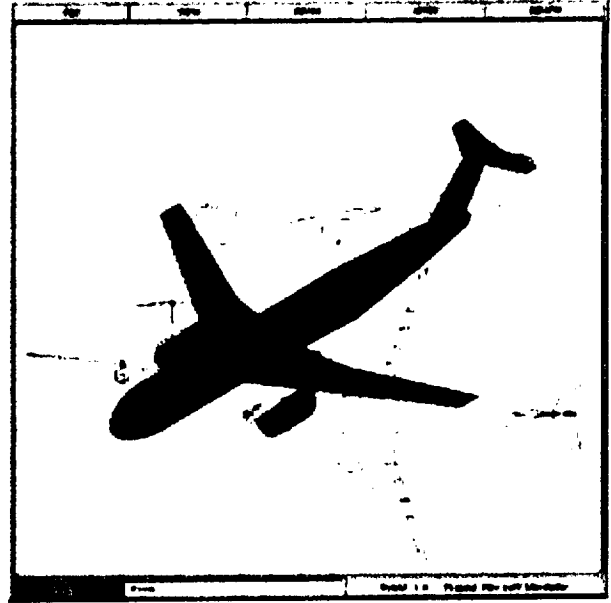


Figure 2. Commercial Transport RAM Model

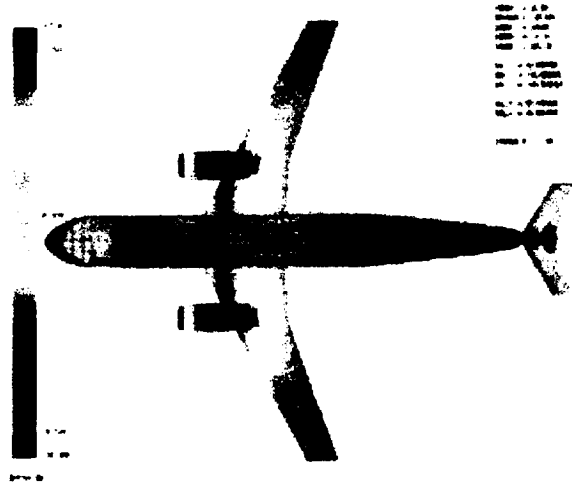


Figure 3. Grayscale Mapping of the Surface Pressure Distribution for the Commercial Transport Model

## Error Controller

Errors in roll rate, pitch rate, and yaw rate responses can be caused by inaccuracies in aerodynamic estimates and model inversion. Unidentified damage or failures can also introduce additional errors. In order to achieve a rate-command-attitude-hold (RCAH) system, a proportional-integral (PI) error controller is used to correct for errors detected from roll rate, pitch rate, and yaw rate ( $p$ ,  $q$ ,  $r$ ) feedback. Table 1 contains the error controller gains used for each axis.

Table 1. Error Controller Gains

	P-Axis	Q-Axis	R-Axis
$\omega_c$	3.5	2.5	2.0
$\zeta_c$	0.707	0.707	0.707
$K_p$	$2\zeta_c\omega_c$	$2\zeta_c\omega_c$	$2\zeta_c\omega_c$
$K_i$	$\omega_c^2$	$\omega_c^2$	$\omega_c^2$

On-Line Learning Neural Networks

The on-line learning neural networks work in conjunction with the error controller. By recognizing patterns in the behavior of the error, the neural networks can learn to remove biases through control augmentation commands. These commands prevent the integrators from having to windup in order to remove error biases. By allowing integrators to operate at nominal levels, the neural networks enable the controller to provide consistent handling qualities.

A two-layer sigma-pi neural network is used for each channel.<sup>6</sup> Inputs into the network consist of control commands, sensor feedback, and bias terms. Table 2 contains the inputs for each input signal category. Normalized inputs are used for the aircraft's altitude ( $h$ ) and airspeed ( $v_i$ ) in order to compensate for dynamic pressure effects.

Table 2. Input Signal Category Elements

	P-Network	Q-Network	R-Network
$C_1$	.1, $v_i, v_i^2, h$	.1, $v_i, v_i^2, h$	.1, $v_i, v_i^2, h$
$C_2$	.1, $p, q, r, p_c, \frac{1-e^{-p}}{1+e^{-p}}$	.1, $p, q, r, q_c, \frac{1-e^{-q}}{1+e^{-q}}$	.1, $p, q, r, r_c, \frac{1-e^{-r}}{1+e^{-r}}$
$C_3$	.1, $\alpha, \beta$	.1, $\alpha, \beta$	.1, $\alpha, \beta$

The vector of basis functions is computed from the inputs in each signal category using a nested kronecker product.<sup>6</sup> Network weights are computed from the error signals using the adaptation law

$$adaption\ law = \frac{1}{2K_i} \int error + \frac{1+K_i}{2K_i K_p} error \quad (3)$$

Multiple techniques are used to prevent integrators and neural networks from trying to compensate for errors during control saturation. Windup protection is used during lateral and directional control saturation.<sup>5</sup> Pseudo-control hedging is used during longitudinal control saturation.<sup>9</sup>

Control Allocation

A daisy-chain control allocation technique is used to ensure that conventional flight control surfaces will be utilized under normal operating conditions. Unconventional flight control surface allocations are only utilized when the primary flight control surface commands exceed the known limits of deflection. Table 3 contains the daisy-chained control allocation scheme for each axis.

Table 3. Daisy-Chain Control Allocation

	Lat.	Dir.	Long.
Primary Allocation	$\delta_{dail}$	$\delta_{drud}$	$\delta_{elev}$
Secondary Allocation	yaw-based roll control	$\delta_{dthr}$	$\delta_{ail}$
Tertiary Allocation	- - -	- - -	$\delta_{thr}$

In the longitudinal axis, figure 4, pitch rate control is normally provided through symmetric elevator deflections. If this command should saturate, then the remaining portion of the command is applied to symmetric ailerons. If the symmetric aileron command saturates, then the remaining portion of that command is applied to symmetric thrust. The symmetric aileron command is limited, by the differential aileron command, so that secondary pitch control does not interfere with primary roll control. Speed control is dropped when symmetric thrust is required for achieving desired pitch control. If the symmetric thrust command exceeds idle or maximum thrust limits, then the remaining portion of the command is used to offset the reference model via pseudo-control hedging.

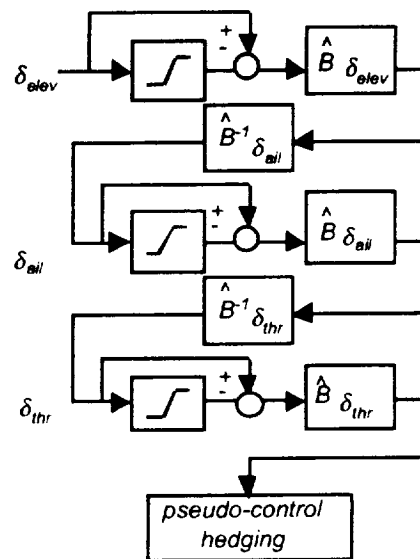


Figure 4. Longitudinal Control Allocation

In the directional axis, figure 5, yaw rate control is normally provided by rudder deflection. If this command should saturate, then the remaining portion of the command is applied to differential thrust. In this case, the rudder command limit is a function of dynamic pressure. The differential thrust command is limited, by the current throttle position, so that secondary directional control does not interfere with primary speed, or tertiary pitch, control. As a result, differential thrust limits are zero if throttles are at idle or maximum thrust. If the differential thrust command exceeds limits, then windup protection is invoked to avoid integrator buildup and neural network adaptation during control saturation.

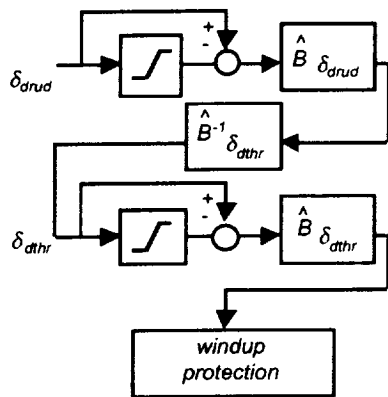


Figure 5. Directional Control Allocation

In the lateral axis, figure 6, roll rate control is normally provided by differential aileron deflections. In this case, differential spoiler control is also slaved to the differential aileron command. Since no other backup roll control source is available, a PCA concept is utilized which incorporates yaw-based roll control. Therefore, if the differential aileron command should saturate, the remaining portion of the command is multiplied by a yaw-based roll control gain ( $K_{ybrc}$ ), and added to the existing yaw rate command. If an aircraft were to lose all flight control surfaces it would be flown under propulsion only control, using a combination of differential and symmetric thrust and yaw-based roll control.

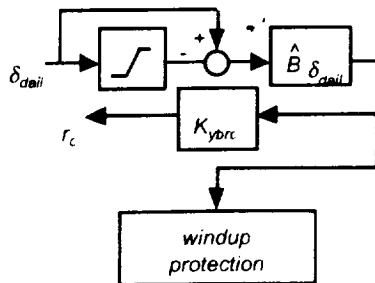


Figure 6. Lateral Control Allocation

## Simulation Tests

The INFPCS system was evaluated on the Advanced Concepts Flight Simulator (ACFS) at NASA Ames Research Center. Test results are presented, under nominal and simulated failure conditions, along with comparisons to conventional flight control systems.

## Simulator Description

The simulator, shown in figure 7, is equipped with a six degree-of-freedom motion system, programmable flight displays, digital sound and aural cueing system, and a 180-degree field of view visual system.<sup>10</sup>

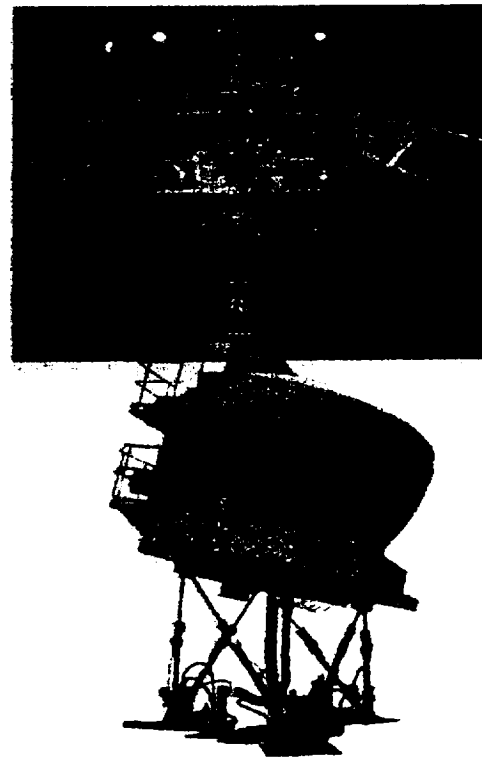


Figure 7. ACFS Simulator

The simulated aircraft, displayed in figure 1, is representative of a mid-size two-engine jet transport with general characteristics of a wide-body, T-tail, low wing airplane with twin turbofan engines located under the wings. The aircraft is based on a Lockheed Georgia Company Commercial transport concept developed in 1983. The physical dimensions are similar to a Boeing 757 aircraft, with flight characteristics representative of a mid-sized jet transport. This particular transport aircraft, designed as a platform for testing advanced concepts, is equipped with active flight controls representative of an advanced fly-by-wire control system.

The Dryden turbulence model provides turbulence RMS and bandwidth values which are representative those specified in Military Specifications Mil-Spec-8785 D of April 1989. The Earth atmosphere is based on a 1976 standard atmosphere model.

### Test Objectives

The purpose of the study was to evaluate the performance of the INFPCS system on a two-engine mid-sized commercial transport aircraft. The objective was to conduct piloted tests and evaluations under nominal and simulated conditions.

### Test Description

The INFPCS system was evaluated by a total of 12 pilots, 6 NASA test pilots and 6 commercial airline pilots (3 commercial airline crews). Test pilots performed select maneuvers and approach and landing scenarios under nominal and simulated failure conditions. Handling characteristics were compared to those of a standard "Open-Loop" cable-driven controller, and a "Conventional" rate-command-attitude-hold (RCAH) fly-by-wire (FBW) controller. Commercial pilots performed full-mission flights, from takeoff to landing, in order evaluate the effectiveness under select operational scenarios. The evaluation criteria was based upon performance measurements, Cooper-Harper ratings, and pilot comments.

Failure conditions consisted of "frozen" flight control surfaces at neutral or offset positions, shifts in the center of gravity, and special controller failures to measure levels of adaptation. The failures used in this evaluation were selected in order to investigate specific control issues, and to represent realistic scenarios encountered in aircraft accidents and incidents involving the loss of some or all flight control surfaces.<sup>1</sup>

### Handling Quality Tests

Handling quality maneuvers were performed in high-altitude flight. Maneuvers consisted of a sequence of bank angle (0°, 10°, -10°, 20°, -20°, 30°, -30°, 0°) and pitch angle ( $\Delta 0^\circ$ ,  $\Delta 5^\circ$ ,  $-\Delta 5^\circ$ ,  $\Delta 10^\circ$ ,  $-\Delta 10^\circ$ ,  $\Delta 0^\circ$ ) gross acquisition tasks, and a fine tracking task presented to the pilot through the flight director. All handling quality maneuvers were performed in light turbulence and clear visibility conditions.

### Baseline Tests

The baseline tests were performed using the Open-Loop, Conventional, and INFPCS controllers under non-failure conditions. Three different INFPCS modes were used in order to evaluate the effects of "learning". The INFPCS modes consisted of (1) INFPCS without adaptation, (2) "untrained" INFPCS

with adaptation, and (3) "trained" INFPCS with adaptation. The trained condition was established by first performing the maneuver with the untrained neural networks and then repeating the maneuver with the trained neural networks.

Figure 8 displays the mean Cooper-Harper Ratings (CHR), along with maximum and minimum ranges, for the lateral axis. Pilots rated all controllers with Level I (CHR of 1-3) or Level II (CHR of 4-6) handling qualities. The Conventional controller had the most desirable ratings, while the INFPCS system without adaptation had the least desirable ratings. Pilots commented that, without adaptation, the INFPCS system was "sluggish" and had a tendency to "overshoot" the target bank angle. The performance of INFPCS improved considerably with adaptation. Pilots described the adaptive system as "more responsive" and "precise".

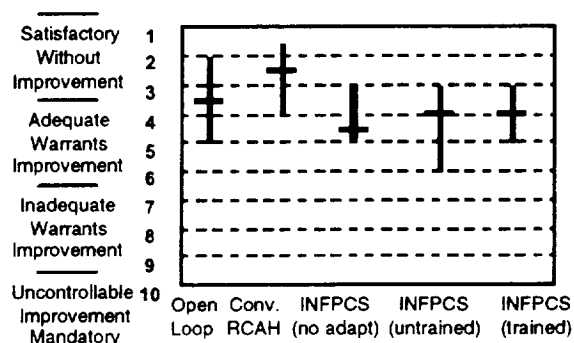


Figure 8. Lateral Cooper-Harper Ratings (No Failure Condition)

Several pilots were able to detect the effects of adaptation when performing the initial maneuver with the untrained neural networks. One pilot even commented that it was difficult to provide ratings for a changing system. As a result, ratings with the untrained neural networks had a tendency to vary, as some pilots applied more weight to the beginning or the ending of the maneuver.

One noticeable adverse effect of adaptation was encountered at the beginning of the initial maneuver with the untrained neural networks. Pilots had a tendency of overshooting the initial bank angle target. In this case, both the pilot and the INFPCS system were trying to compensate for the "sluggish" system. However, by the completion of the maneuver, the neural networks were sufficiently trained, allowing pilots to perform additional maneuvers with minimal compensation.

Figure 9 displays the mean ratings, along with maximum and minimum ranges, for the longitudinal axis. Pilots rated all controllers with Level I or Level II handling qualities. The trained INFPCS controller had the most desirable ratings, while the INFPCS system without adaptation had the least desirable ratings.

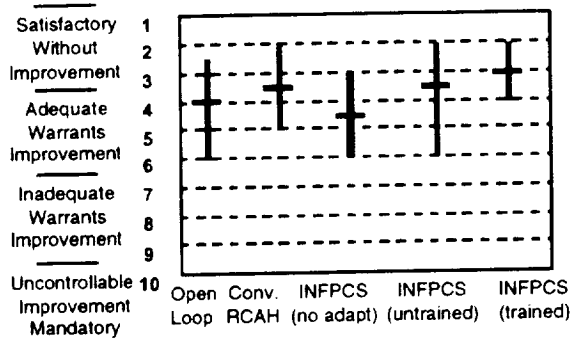


Figure 9. Longitudinal Cooper-Harper Ratings (No Failure Condition)

During the initial pitch maneuver, many pilots discovered another adverse effect of adaptation. Pilots commented that there appeared to be a slight pitch-roll coupling, especially during the acquisition of the first pitch target. By the completion of the maneuver, the pitch-roll coupling had appeared to dissipate. While this effect occurred during the pitch maneuvers, the degradation in performance was usually reflected in the lateral ratings.

Further investigation uncovered that this coupling phenomenon was caused by the selection of neural network inputs (Table 2). The body-axis rates ( $p$ ,  $q$ ,  $r$ ) were used as inputs, into each neural network ( $P$ -Network,  $Q$ -Network,  $R$ -Network), in order to compensate for potential cross-axis effects that might occur. However, performing repeated bank angle maneuvers caused the neural networks to identify a pattern between roll rate and pitch error. This pattern was stimulated by the cross-axis correlated commands generated by the level-turn compensation system.

### Controller Failure Tests

An INFPSC "Controller Failure" was used to measure levels of adaptation. In this case, the pre-trained neural network was initialized with no prior knowledge of the aircraft's stability and control derivatives. Essentially, the pre-trained neural network was initialized with a signed and scaled identity control matrix (B-matrix), and a zero stability matrix (A-matrix).

During the Controller Failure tests, the effect of adaptation became more apparent. Figures 10 and 11 displays roll rate and pitch rate errors respectively, during a sample test case when performing sequential sets of maneuvers. The first set of maneuvers, performed without adaptation, contains the largest errors. Adaptation is then used during the second set of maneuvers, starting with untrained neural networks. The magnitude of the error continues to reduce as the maneuver is repeated a third time, representing trained neural networks. Pilots commented that there was a "big difference" in performance, as lateral ratings

improved from 6.7 to 3.8 CHR, and longitudinal ratings improved from 6.6 to 4.2 CHR.

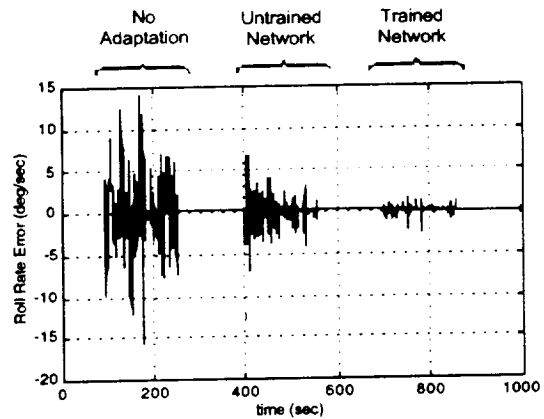


Figure 10. INFPSC Roll-Rate Errors (Controller Failure)

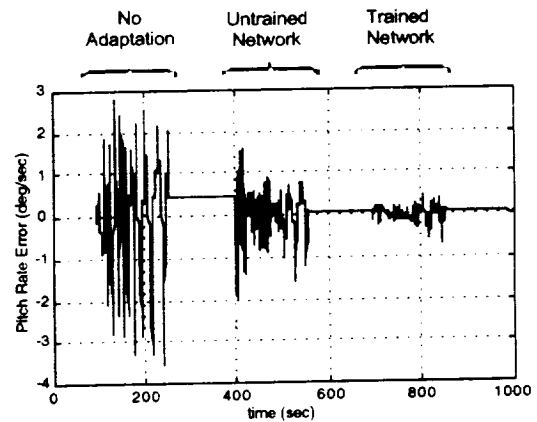


Figure 11. INFPSC Pitch-Rate Errors (Controller Failure)

### Dead-Band Adaptation Tests

One important aspect for consideration, when utilizing a daisy-chain control allocation scheme, is to determine how the system will respond to failures that result in control allocation dead-bands. While fault detection and isolation systems can be used to provide the necessary information for bypassing dead-bands, the possibility of non-detection must also be considered. By freezing both the left and right elevators at their neutral position, the primary means of pitch control of an aircraft is lost. Since the INFPSC system does not command symmetric ailerons until the elevator command saturates, this "Frozen Elevator" can be used to create a dead-band in the longitudinal axis.

The Frozen Elevator tests were only performed with the INFPSC system, since the other controllers did not provide alternate pitch control. As the integrator in the error controller wound up and down to overcome

the dead-band, there was a resulting delay in the pitch response. Without adaptation, delays in pitch response were on the order of 7 seconds. With neural network adaptation, delays were reduced to approximately 2 seconds. While the ratings for the longitudinal gross acquisition task only improved slightly, from 4.4 to 3.4 CHR, the fine tracking accuracy improved significantly by a 65% reduction in the flight director tracking error.

### Out-of-Trim Tests

Another important issue for consideration is the determination of how a system will respond to out-of-trim conditions. This issue was evaluated, in the longitudinal axis, by simulating a "Runaway Stabilizer Trim" to the full nose-down position. In this case, there was sufficient control authority in the elevator to compensate for the out-of-trim stabilizer. A lateral out-of-trim condition was evaluated by shifting the center of gravity (CG) laterally 7 feet to the right. Under certain flight conditions, particularly encountered during approach configurations, this "Lateral CG Offset" would cause the ailerons to go in and out of saturation, requiring yaw-based roll control.

While sufficient control authority remained to stabilize and control the aircraft in each case, the Open-Loop controller typically resulted in an uncontrollable condition. In the case of the Runaway Stabilizer Trim, the aircraft typically lost several thousand feet before the pilots were able to stabilize the aircraft. However, the amount of force required for maintaining level flight prevented the execution of handing quality maneuvers. In the case of the Lateral CG Offset, there was normally insufficient reaction time available to prevent the aircraft from departing to an inverted state.

Both the Conventional and INFPCS controllers were able to stabilize the aircraft without significant pilot compensation. The integrators, inherent in both systems, were able to generate the command biases required to compensate for the out-of-trim condition. However, pilots were able to detect a noticeable difference when performing the gross acquisition maneuvers.

Figure 12 displays the mean longitudinal ratings, along with maximum and minimum ranges, for the Runaway Stabilizer Trim. In this case, the Conventional controller had a tendency of being slightly faster in the pitch-down direction, and "very sluggish" in the pitch-up direction.

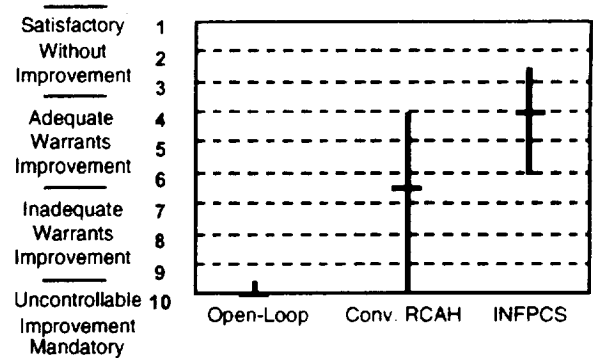


Figure 12. Longitudinal Cooper-Harper Ratings (Runaway Stabilizer Trim)

Figure 13 displays the mean lateral ratings, along with maximum and minimum ranges, for the Lateral CG Offset. In this case, the Conventional controller had a tendency of being faster in the bank-right direction and slower in the bank-left direction. Pilot ratings varied, as the magnitude of this effect was dependent upon aggressiveness and technique during the maneuver.

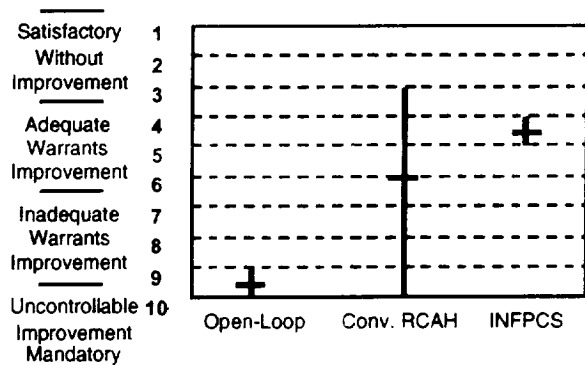


Figure 13. Lateral Cooper-Harper Ratings (Lateral CG Offset)

The INFPCS system was evaluated with adaptation, starting with untrained neural networks. For both the Runaway Stabilizer Trim and Lateral CG Offset, the overall performance was described as being "more balanced", even though secondary control allocations were rarely utilized. Once trained, the neural networks were able to provide consistent handing qualities by generating the necessary command biases to enable the integrators to unwind.

### Approach and Landing Tests

Approach and landing test were used to evaluate the INFPCS system under realistic flight critical operations. The scenarios began in straight and level flight, 2,000 feet above ground level, with an

airspeed of 200 knots. The aircraft was initialized flying parallel to the runway, 15 nautical miles from the touchdown point, with a 4,500 foot lateral offset to the right. Weather conditions consisted of varying turbulence, wind and visibility conditions. A runway incursion was also introduced in order to force a "surprise" sidestep maneuver.

### Tail Failure Tests

In cases involving flight control surface failures, the area most commonly effected was the tail of the aircraft.<sup>1</sup> As a result a "Tail Failure" was used to create dead-bands in both the longitudinal and directional axes. In this case, both elevators and the rudder were frozen at their neutral positions, and the stabilizer was frozen at the trim position.

Pilots performed approach and landing maneuvers with a Tail Failure using the Conventional and INFPCS controllers. Half of the pilots were able to achieve successful landings with the Conventional controller by manually overriding the throttles to control pitch. All pilots were able to achieve successful landings with the INFPCS controller. Figures 14 displays a sample approach of one of the successful landings using the Conventional controller, along with the same approach using the INFPCS controller.

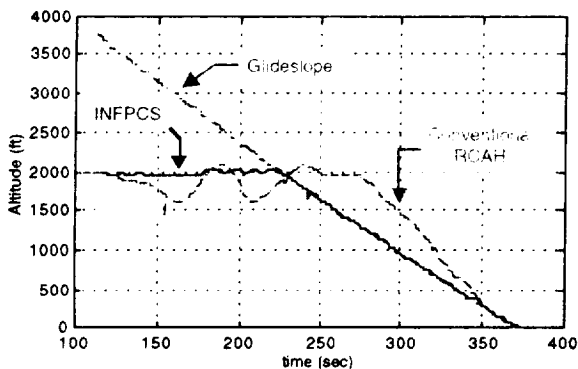


Figure 14. Altitude During Approach (Tail Failure)

While gross control was possible by manually controlling throttles with the Conventional controller, the constant "ballooning in pitch" made glideslope tracking difficult. Glideslope tracking performance improved dramatically using the INFPCS controller. However, the dead-band in longitudinal control did affect flare performance. The mean sink rate at touchdown was degraded, from a baseline of -3 ft/sec, to -9 ft/sec. However, using the Conventional controller, the mean sink rate was -12 ft/sec. The addition of moderate turbulence did not significantly affect the performance using the INFPCS controller, however pilots did comment that the workload was "manageable but higher".

During the Tail Failure the primary means of pitch control was provided by symmetric aileron commands, however symmetric thrust commands was also utilized upon aileron command saturation. While symmetric thrust commands were found to provide a slight benefit during large pitch maneuvers, the slow engine response resulted in disruptive speed control during high frequency pilot commanded pitch corrections. In some cases, as in Figure 15, continuous minor pitch corrections caused the aircraft to land several knots above the target landing speed (145 knots). However, there was still an improvement in speed control, over manually controlling throttles with the Conventional controller.

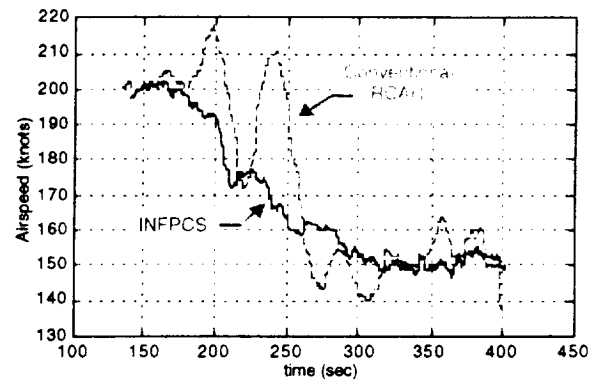


Figure 15. Airspeed During Approach (Tail Failure)

The slow engine response time also prevented differential thrust commands from performing effective yaw-dampening. This problem was compounded by the presence of the directional dead-band. However the subtle bank maneuvers required for localizer tracking, prevented dutch-roll excitation. In the event of a large bank maneuver, the attitude-hold portion of the lateral control system helped to dampen the oscillation.

### Control Allocation Transition Tests

In order to test the transition when allocating between two different longitudinal control sources, the Runway Stabilizer Trim was compounded by also freezing the right elevator in the neutral position. This resulting "Combination Failure" required the remaining left elevator to go in and out of saturation. This would also produce a pitch-roll coupling effect due to the "split elevators". Since aerodynamic data was not available for simulating this coupling effect, vortex-lattice code was used to generate the necessary data approximations.

Pilots performed approach and landing maneuvers with the Combination Failure using the Conventional and INFPCS controllers. Only one pilot was able to land the aircraft with the Conventional

controller. The pilot manually used throttles and spoilers to obtain additional pitch control, and landed the aircraft at 250 knots. One difficult aspect of performing this maneuver was that the pilot response time had to be within a few seconds after the failure occurred. With the INFPCS controller, all pilots were able to achieve a safe runway landing. The mean sink rate at touchdown was  $-4$  ft/sec. Pilots described the failure as "transparent", even when performing a "surprise" side-step maneuver at an altitude of 500 ft because of a runway incursion.

Figure 16 displays the position of the left and right elevator during the approach. Since the right elevator was failed, and the stabilizer was frozen in the maximum nose-down direction, the left elevator had a large bias in the negative, or pitch-up, direction. As a result, the left elevator went in and out of saturation (at  $-25$  deg) during the approach. This allowed the daisy-chain to be evaluated when allocating between the left elevator and symmetric ailerons.

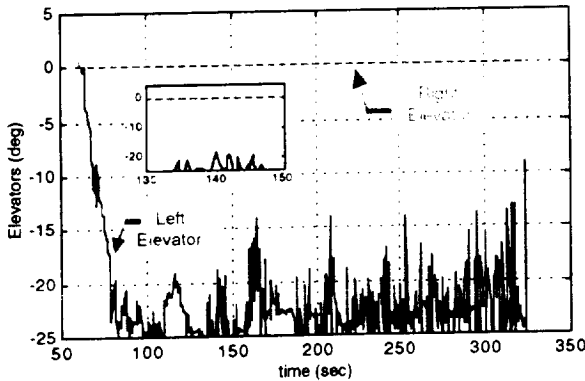


Figure 16. Elevators During INFPCS Approach (Combination Failure)

Figure 17 displays the position of both ailerons during the approach. There is a slight bias between the two ailerons in order to compensate for the rolling moment caused by the split elevators. When the left elevator reaches saturation, the remaining portion of the acceleration command is applied to both the left and right ailerons in the negative, or pitch-up, direction. Since the pitch authority of the ailerons is substantially lower than the elevators, the ailerons are driven to larger deflections.

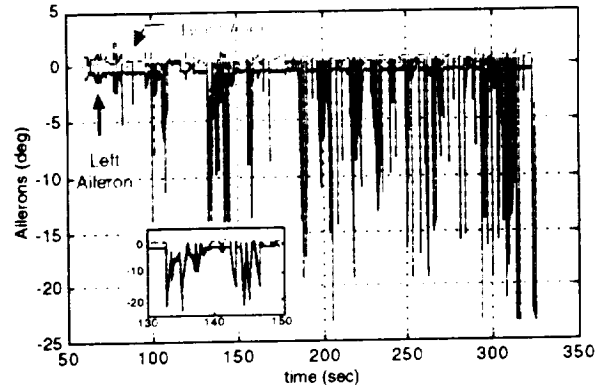


Figure 17. Ailerons During INFPCS Approach (Combination Failure)

### Yaw-Based Roll Control Tests

The Lateral CG Offset was used to test the effect of yaw-based roll control. During the approach the ailerons would begin to saturate as the aircraft decelerated to approach speed. Pilots performed this approach and landing maneuver using the Conventional and INFPCS controllers. Half of the pilots were able to achieve a successful landing, with the Conventional controller, through manual rudder manipulation. All of the pilots were able to achieve successful landings with the INFPCS controller.

While the mean INFPCS ratings improved from 8.6 to 5.4 CHR, pilots commented that the yawing moment was still "very disconcerting". One contributing factor was that the yawing moment was not as easily anticipated, when compared to applying manual rudder inputs. However, with automatic yaw-based roll control, pilot response time became less critical when the ailerons entered saturation. The INFPCS controller also utilized differential throttle inputs, when the rudder command saturated, during quick banking maneuvers to the right.

### Control Saturation Tests

A "Hard-over Rudder" was used to evaluate the effects of control saturation in the directional axis. In this case, there was insufficient control authority using differential thrust to compensate for the rudder displacement. However there was sufficient aileron control authority to maintain lateral control.

Pilots performed approach and landing maneuvers with the Hard-over Rudder using the Conventional and INFPCS controllers. All pilots were able to land the aircraft with no significant difference in performance between the two controllers. While the INFPCS system applied automatic differential thrust to reduce the sideslip caused by the rudder, pilots were able to achieve similar results through manual throttle manipulation.

## Operational Scenario Tests

The commercial airline pilots performed two standard commercial flights using INFPCS as the flight controller. The simulations included pseudo aircraft and air traffic control. The first scenario consisted of a short flight, from Sacramento (KSMF) to San Francisco (KSFO), with a single point failure. During the flight, the elevators were failed at the neutral position during the cruise segment of flight just prior to reaching the top of descent. The second scenario consisted of a longer flight, from San Francisco (KSFO) to Los Angeles (KLAX), with cascading failures. During the cruise segment of the flight, the stabilizer experienced a runaway trim to the full nose-down position. Shortly after beginning the descent, the right elevator became frozen at the neutral position. Finally, towards the end of the descent, the rudder became frozen with a 3 degree offset to the right.

All of the crews were able to achieve successful runway landings. While only half of the pilots noticed the effects of adaptation, all pilots expressed approval over the system's robustness to failures. "It makes a very difficult situation much easier", resulting in "little difference in normal flying". One potential implementation aspect was encountered when using a flight-level-change (FLCH) mode during descent. In this energy management mode, pitch controls speed while the auto-throttles are disengaged after going to idle. As a result, propulsion control was disabled during a large portion of the flight.

## Conclusions

In the event of damage or failure, an aircraft's response can change to the point of essentially becoming a new aircraft. Since conventional transport aircraft have limited additional control power available, alternate control allocation schemes may be necessary. The INFPCS system demonstrates the effectiveness of using neural networks to not only adapt to changes in aircraft dynamics, but also to adapt to different control allocation schemes. While a daisy-chain approach was used in this evaluation, alternate schemes incorporating system identification or fault detection and isolation may also be utilized.

While propulsion control was demonstrated to provide additional control authority when necessary, propulsion-only based control was determined to require an outer-loop control interface such as an autopilot. However enabling autopilot interfaces, such as the ones used for PCA, would require dead-band elimination and alternate or adaptive reference models to reduce command frequencies to match slower engine response. Potential areas of future research include the utilization of indirect adaptive schemes, in order to identify control dead-bands, an adaptive outer-loop control.

## References

- [1] Burcham, Frank W., Jr., Trindel A. Maine, C. Gordon Fullerton, and Lannie Dean Webb, *Development and Flight Evaluation of an Emergency Digital Flight Control System Using Only Engine Thrust on an F-15 Airplane*, NASA TP-3627, Sept. 1996.
- [2] National Transportation Safety Board, Aircraft Accident Report, PB90-910406, NTSB/ARR-90/06, United Airlines Flight 232, McDonnell Douglas DC-10, Sioux Gateway Airport, Sioux City, Iowa, July 1989.
- [3] Burcham, Frank W., Jr., John J. Burken, Trindel A. Maine, and C. Gordon Fullerton, *Development and Flight Test of an Emergency Flight Control System Using Only Engine Thrust on an MD-11 Transport Airplane*, NASA TP-97-206217, Oct. 1997.
- [4] Kaneshige, John, John Bull, Edward Kudzia, and Frank W. Burcham, *Propulsion Control with Flight Director Guidance as an Emergency Flight Control System*, AIAA 99-3962, August 1999.
- [5] Kaneshige, John, John Bull, and Joseph J. Totah, *Generic Neural Flight Control and Autopilot System*, AIAA 2000-4281, August 2000.
- [6] Rysdyk, Rolf T., and Anthony J. Calise, *Fault Tolerant Flight Control via Adaptive Neural Network Augmentation*, AIAA 98-4483, August 1998.
- [7] Norgaard, M., Jorgensen, C., and Ross, J., *Neural Network Prediction of New Aircraft Design Coefficients*, NASA TM-112197, May 1997.
- [8] Totah, Joseph J., David J. Kinney, John T. Kaneshige, and Shane Agabon, *An Integrated Vehicle Modeling Environment*, AIAA 99-4106, August 1999.
- [9] Johnson, Eric N., Anthony J. Calise, and Hesham A. El-Shirbiny, *Feedback Linearization with Neural Network Augmentation Applied to X-33 Attitude Control*, AIAA 2000-4156, August 2000.
- [10] Blake, Matthew W., *The NASA Advanced Concepts Flight Simulator: A Unique Transport Aircraft Research Environment*, AIAA-96-3518-CP.